Response from current and regular/irregular waves on a typical polyethylene fish farm

Are Johan Berstad & Harald Tronstad
Aquastructures Postboks 1223 – Pirsenteret 7000 Trondheim Norway
www.aquastructures.no. are.berstad@aquastructures.no, harald.tronstad@aquastructures.no

ABSTRACT:

A new technical standard, NS 9415 has been introduced to the fish farming industry in Norway. Several technical projects are currently being carried out to enhance the technical foundation for improvements of NS 9415. In this paper work in one of these projects is presented.

Design codes do in general describe the relation between the maximum wave height to be used in a design wave approach and the significant wave height. NS 9415 does likewise. Due to the large extension of typical fish farm facilities, the use of a design wave approach may be more conservative compared to structures where one wave cover the structure. The importance of this issue is closely correlated to the relative importance of current and waves and the combined effect of these two load components.

The case study presented in this paper considers the responses from waves and current within a typical polyethylene fish farm configuration Analysis using both regular and irregular waves, combining load cases consisting of both current and waves has been carried out and is presented. The results show that both waves and current should be accounted for, and that design loads for parts of the mooring system may be reduced by using irregular waves. However for the general case, the present relation between regular and irregular waves seems reasonable.

1 INTRODUCTION

As of April 1st 2004 a Norwegian Standard NS 9415 was introduced to the offshore fish farming industry in Norway. This was the first technical standard world wide to be applied for such facilities.

The standard, NS 9415 specify technical criteria fish farm facilities need to comply with in order to be acknowledged for use in Norway.

Since NS 9415 is new, there is little experience of applying it to practical fish farm facilities. As part of a joint industry effort, Aquastructures as a certification body within the industry have initiated a research project to enhance both the analytical and empirical basis of the standard.

There have recent years been several research efforts on fish farm facilities. Fredheim and Faltinsen (2003) have proposed a model to calculate the response of net structures. In this model the wake behind meshes is derived and hence fluid velocities, making it possible to account for velocity reduction behind the mesh analytically. So far this has generally been based on empirical values (e.g. Løland 1991). Lader et. al. (2003) use a time domain drag load approach similar to the present for waves and current, but have an alternative formulation for the net structure elements as well as for the drag and lift force. Vikestad and Lien (2005) proposed a simplified formula for the relation between current velocity and forces in the mooring system. Berstad et. al. (2005) presented case studies of volume calculations and forces on both floaters and mooring system. Fredriksson et al (2003) has compared calculations with measurements for a type of fish farm where a linearized approach was applicable allowing for them to carry out a frequency domain analysis.

Typical fish farm structures in the market today have too large deflections when exposed to wave and current forces that linearized approaches are not applicable in order to account for the highly flexible structures interacting with fluid forces in a hydroelastic manner.

Generally, current induced forces have been considered important for polyethylene based fish farm systems. However, some related questions have been raised:

- How important are wave forces compared to current induced forces?

• Is it too conservative to use a design wave approach for derivation of wave forces?

This paper presents a case study on a polyethylene based fish farm system as shown in Figure 1 investigating the above queries. The case study represents a typical fish farm system operating in Norway today. In addition, forces in the different mooring components due to current will be compared to the formula presented by Vikestad and Lien (2005).

The algorithm and softwaretool used for the calculations is outlined in Berstad et al (2004).

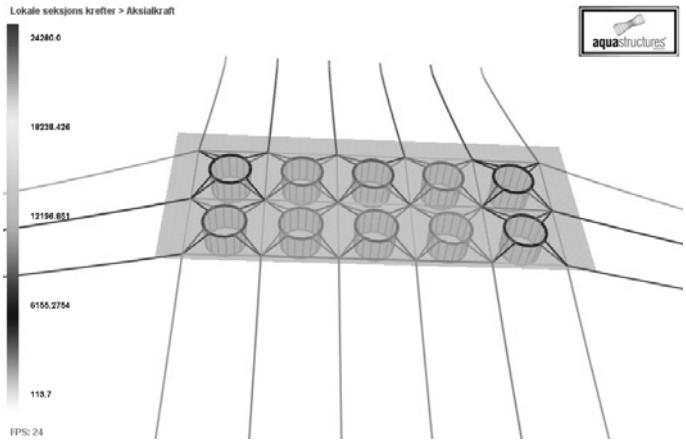

Figure 1 Fish farm used as case study

2 POLYETHYLENE FISH FARMS

Fish farms with polyethylene floaters are typically built up with a flag shaped fishnet with weights in the areas close to the bottom and a floater giving the buoyancy as seen in Figure 2. A mooring system is attached to the floater. Most commercial fish farms consist of several floaters as similar to the case seen in Figure 1. Systems with up to 20 and 30 cages exist. Typical systems based on steel cages may be seen in Berstad et al (2004).

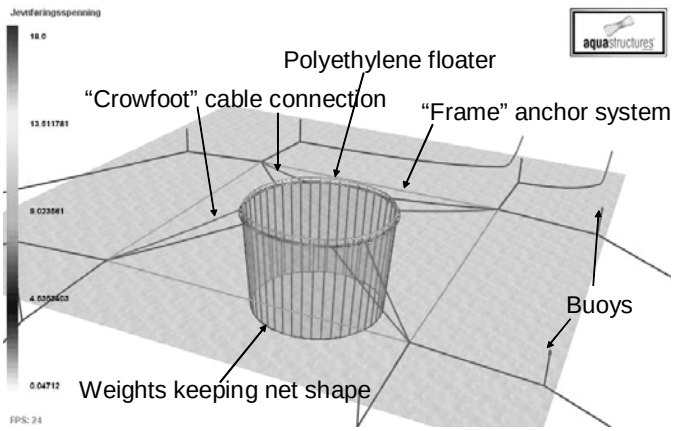

Figure 2 Usual mooring system for polyethylene based fish farms

3 CASE STUDY

For this case study a 10 cage fish farm system is used. A each cage there are two polyethylene rings. They are modeled in a simplified manner using one ring with material, cross sectional and buoyancy parameters representing both inner and outer ring.

The floaters are modeled with beam elements accounting for large geometric deformations (e.g. Halse, 1997). The polyethylene pipes have a diameter of 315 mm and a thickness of 17 mm. Hand rails and clamps are not considered. The floater has a Young's module of 0.8 GPa and a Poisson's coefficient of 0.3. The mass density is 950 kg/m^2. The water line is located 130 mm. above the bottom of the floaters at static equilibrium. The Hydrodynamic model has been simplified to an oval section with the same water plane area and buoyancy as two circular sections.

Figure 3 shows key data for the mooring system. The system is symmetric about a vertical plane trough the centre point of the mid cages in the y- direction as seen in Figure 3. All components in the mooring system are modeled with bar elements.

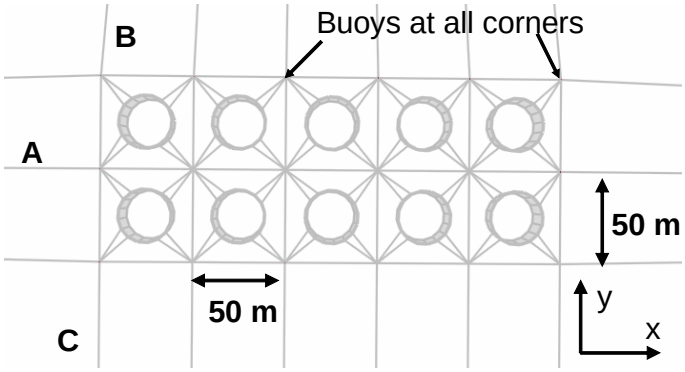

Figure 3 Key data for the mooring system

There are 3 mooring cables of type A (see Figure 3) both left and right. They have a horizontally projected length of 200 meters and a depth of 50, 60 and 73 meters from bottom to top in Figure 3. In addition there is 25 m, 36 mm bottom chain along bottom springs. The mooring cables of type B have a horizontally projected length of 200 meters and a depth of 80 meters with 20 meters chains along the bottom. The mooring cables of type C have a total length of 250 meters bolted to shore. Each has a weight of 1.5 tonnes 30 meters of shore.

All mooring cables are standard polypropylene ropes with a diameter of 48 mm. The Young's module is 2GPa. The square frame part of the mooring

system is located 5 meters below the surface. There are 18 linear surface piercing buoys at each corner of the mooring frame having a water plane area of 0.4 m^2 in the inner region and 1 m^2 at the corners pointing offshore (at the attachment of both type A and B moorings). The density of the polypropylene cables is set to 950. A relative weight in water of 6 N per meter is added.

The fish cage net is modeled with membrane elements, 16 elements in the horizontal and 4 elements in the vertical direction. There are 16 vertical net staves which are modeled with bar elements. The vertical net staves have a Young's module of 2.0 GPa and a diameter of 16 mm. Considering each twine of the net separately, the net itself has a Young's module of 1.0GPa. The diameter of each twine is 2 mm. The meshes are square and the length between knots is 25 mm. Marine fouling is added such that the solidity including fouling is 0.25. Both the net and the net staves are not assumed to have any relative weight in the water.

The net is 20 meters deep and the bottom of the net is not included in the computer model. The weight at the bottom of the net keeping the shape in waves and current is introduced by a filled polyethylene ring. As default this component has a relative weight in water of 20 kg/m in total (the full mass is 35 kg/m). The bottom ring is a 180 mm PE pipe with a thickness of 32 mm. The ring is modeled as a beam. The net is modeled slightly conical such that the circumference of the bottom ring is 81.7 meters.

The method used to carry out the time series simulations of the largely hydroelastic response is outlined in Berstad et al (2004).

For bar elements the Morison formulae is used with the cross flow principle (see. e.g. Faltinsen 1990). The load application to membranes is analogous to the Morison approach used for cables. The present calculations follow the approach of Tronstad (2000).

A reduction coefficient r, is introduced for net structure or part of net structure located behind other net structures (See e.g. Løland 1991).

$$r=1.0 -0.46*Fac \quad (1)$$

where

$$Fac =0.04+(-0.04+0.33Sn+6.54S_n\text{^}2-4.88S_n\text{^}3)*cos(\alpha) \quad (2)$$

where S_n is the solidity of the net and α is zero if the current velocity is normal to the net.

When Morison loads are applied, both the mass of the structure as well as added mass in the cross sectional plane is accounted for. Due to the large deflections occurring, the added mass is nonlinear. Hydrodynamic loads are applied to the floaters meaning that diffraction and radiation is accounted for as described in Berstad et al (2005).

The mooring cables have pretension. In the type A and B mooring cables, tension at static equilibrium is in the range of 20-25 kN. For the type C moorings it is approximately 20 kN. In the frame the pretension varies from 10-20 kN and in the crowfoot type mooring it ranges from 1-9 kN.

A coordinate system is defined such that the *x*- and *y*- axis runs parallel with the mooring as shown in Figure 3.

4 RESULTS AND DISCUSSION

In the graphs in this section the moorings will be named as shown in Table 1

Table 1 Notations used in results for the various parts of the mooring system

Name	Notation
Moorings left and right in Figure 3	A
Moorings to deep side (up) in Figure 3	B
Moorings to shore side (down) in Figure 3	C
Vertical net staves (within the net)	D
Crowfoot type mooring	E
Frame	F

The reported force in this paper will refer to the maximum force in the type of mooring referred to.

4.1 *Forces in the moorings from current*

Vikestad and Lien (2005) proposed a simplified formula for the relation between forces in the mooring and the current velocity, where the resulting forces in the mooring system could be approximated as being linear with respect the current velocity U.

Analysis on the case study has been carried out with various current and wave directions.

Figure 4 and Figure 5 shows the relation between current velocity and maximum axial force in the moorings (A-F). As seen from the figures there will be a range where the pretension is of importance. It is noted that the pretension is only of significant importance in a current range where the mooring on the shaded side is not offloaded.

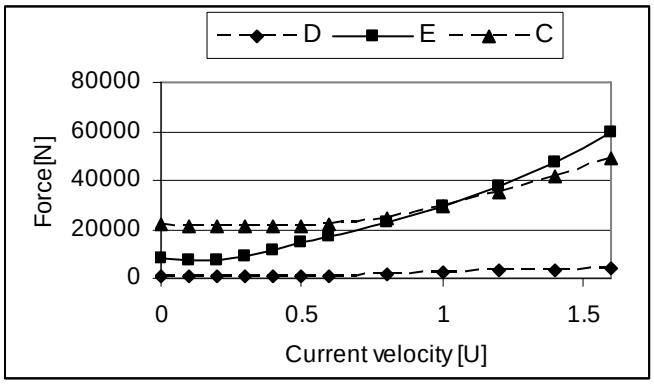

Figure 4 Forces in mooring D, E and F

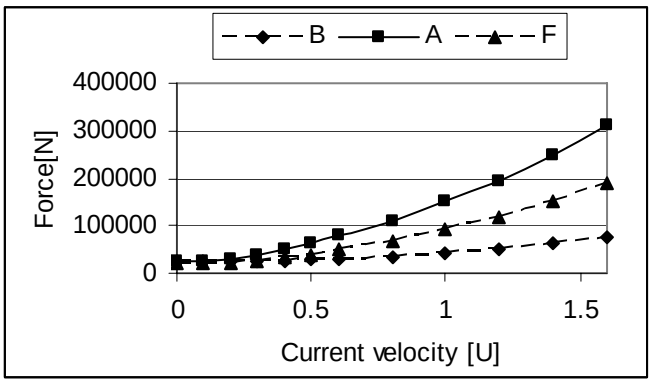

Figure 5 Forces in moorings A, B and F

As seen from Figure 4 and Figure 5 the mooring cable type A are most loaded. This is plausible since these moorings are located upstream. Figure 6 shows the forces in mooring A compared to a linear and a quadratic function originating in the origin and ending at the same force level at U = 1.6.

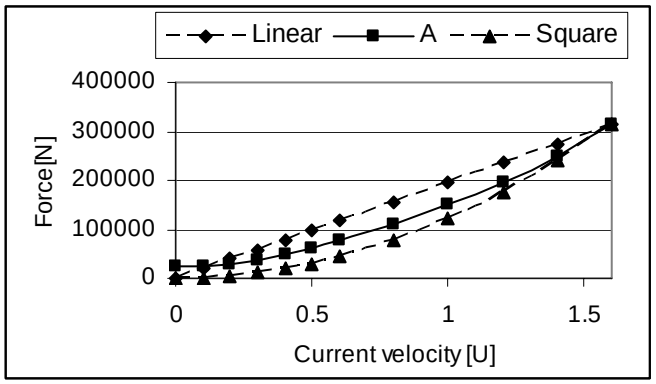

Figure 6 Axial forces as function of current velocity

As seen from Figure 6 the relation between current velocity and mooring forces falls in between a linear and squared response pattern. This is consistent with the used load formulation. Vikestad and Lien (2005) use a formulation based on empirical results by Aarsnes et .al. (1990). We have in the present analysis used the cross flow approach considering each twine separately as in Tronstad (2000). For a typical fish farm facility the net will consist of equally spaced vertical and horizontal twines. For the vertical twines there will be an increased lift component and decreased drag component as the mesh deform. However there will be a drag term for the horizontal twines where the reduction in drag will not be as significant. This will also be the case for the bottom ring. This may give some different results compared to Vikestad and Lien (2005)

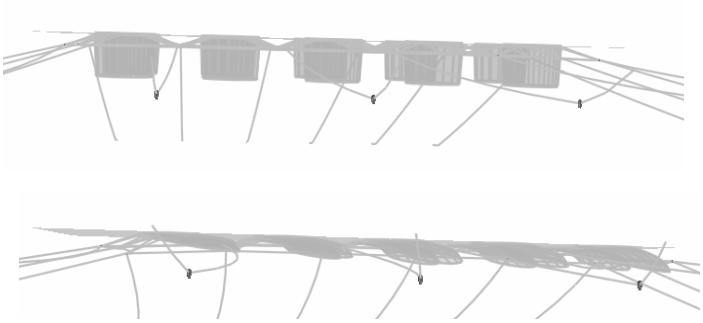

Figure 7 Initial and deformed shape respectively

From Figure 7 it can be noted the strong deformation in the nets with a current velocity of 1.4 m/s. As seen from this figure the deformation is strongest in the nets upstream. This is due to the reduction in current velocity experienced further down the chain due to shading.

4.2 *Current and waves*

How to handle current in combination with waves for design of fish farms is assessed in NS 9415 (NAS 2003).

The most important load component for the whole system is drag loads introduced to the nets in the cages. In a simplified manner these forces can be expressed as

$$F = KC_d \, |U_{rel}| U_{rel} \qquad (3)$$

where U_{rel} is the relative difference in the velocity between the structure and the fluid. KC_d is a factor including the drag coefficient C_d and factors depending on fluid density and angle of attack combined in K. In the above equation

$$U_{rel} = U_{cur} + U_{wave} - V_{struc} \qquad (4)$$

Where U_{cur} is the current velocity, U_{wave} is the fluid velocity introduced by the wave field riding on top of the current field and V_{struc} is the velocity of the structure. Due the nonlinear response from the loads time domain simulations need to be carried out for given sets of current and waves. For the practical calculations this is carried out by first obtaining static equilibrium. Then a steady state solution is obtained for current. Then one wave cycle is used to

build up the wave amplitude. Then two consecutive waves are simulated.

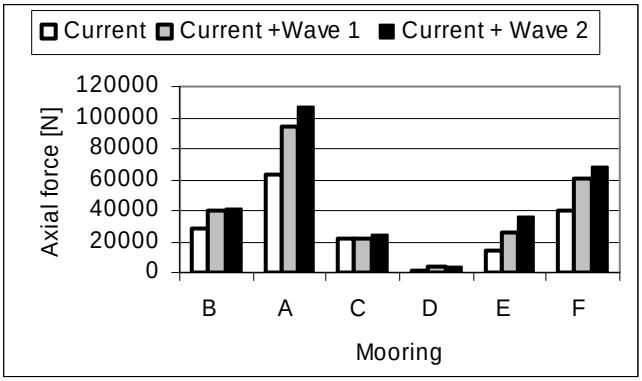

Figure 8 Forces in mooring in current and waves

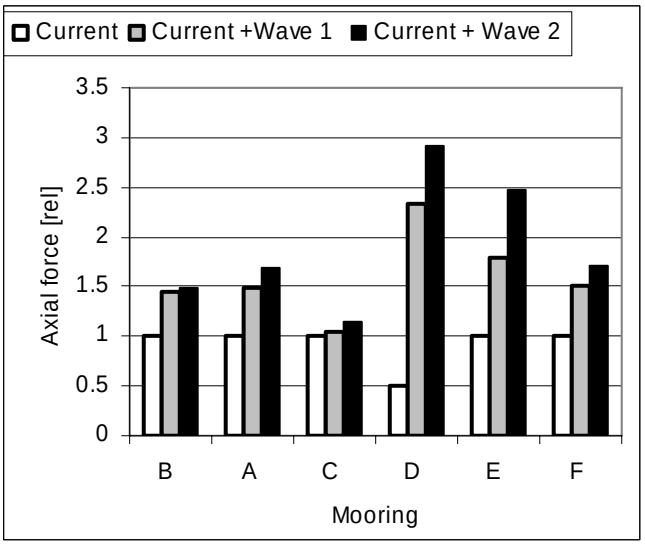

Figure 9 Increase in forces relative to forces with current only

The combination of current and waves investigated is this case study is given in Table 2. These wave conditions represent typical conditions many such facilities are experiencing. Most facilities have a design current of less than 0.5 meters whereas the wave height can be both larger and smaller than the investigated case. Current is assumed to have a uniform distribution with airy waves "riding" the current field. H_{max} is defined as 1.9 Hs.

Table 2 Load cases investigated

Case	Hmax [m]	Period [s]	Wave angle [deg.]	U [m/s]	Current angle [deg.]
1	3.17	4.23	-45	0.5	-10
2	3.8	5.1	-45	0.5	-10
3	3.17	4.23	-45	0.5	-45
4	3.8	5.1	-45	0.5	-45
5	3.17	4.23	-90	0.5	-80
6	3.8	5.1	-90	0.5	-80

As seen from Equation 3 and 4 the force will roughly be depending on the difference between the wave and current velocity and the structural velocity. Loads are applied such that first current is introduced then waves are applied. During the first wave cycle the wave amplitude is increased from 0 to H_{max}, then 2 wave cycles are run with H_{max}.

Figure 8 shows forces in mooring with waves and current from load case 1 and 2 in Table 2. Results are compared to results for current only

Figure 9 shows the same results as Figure 8 but in this case the results are presented relative to results for current only. As seen from the figure all mooring cables experience an increase in the forces when waves are applied. Note that Mooring C is located on the sheltered side towards shore. In mooring D (net staves) the forces will increase 7.5 times meaning that waves are the most important load component for forces in this part of the structure. (Note that the reference value for this load case is 0.5). This agrees with experience that increased waves and increased buoyancy leads to more fatigue in the upper part of the net. For the crowfoot type cables the forces are more than doubled and for the other elements forces are increased from 50 – 70 %.

Figure 10 and Figure 11 shows the same as Figure 8 and Figure 9 but for load condition 3 and 4

The results in Figure 10 and Figure 11 show the same general trend as the results in Figure 8 and Figure 9. Note that the response due to current only will vary due to different current direction.

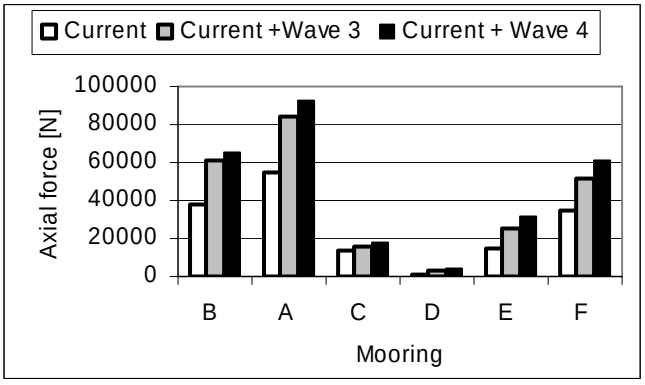

Figure 10 Forces in mooring in current and waves

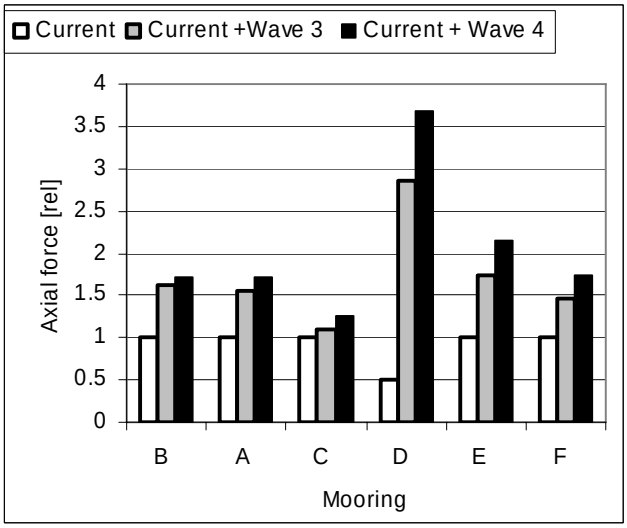

Figure 11 Increase in forces relative to forces with current only

Figure 12and Figure 13shows the same as Figure 8 and Figure 9 for load case 5 and 6.

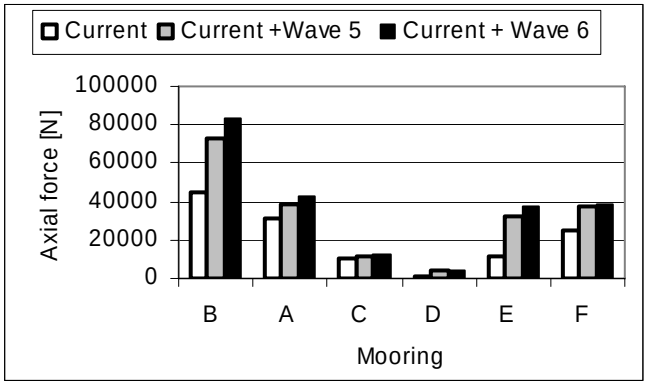

Figure 12 Forces in mooring in current and waves

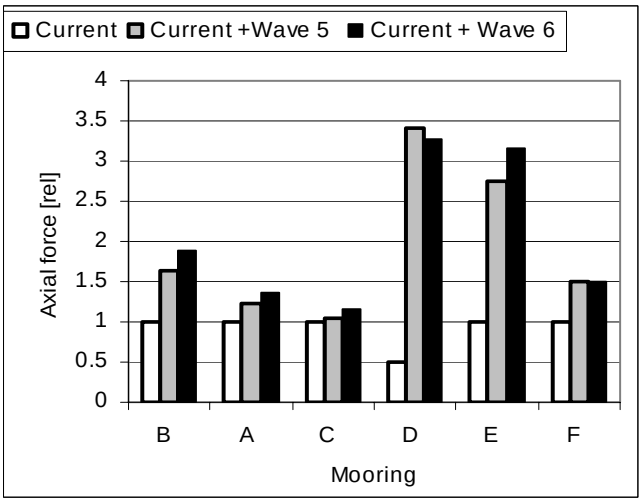

Figure 13 Increase in forces relative to forces with current only

The results in Figure 12 and Figure 13 show the same general trend as the results in Figure 8 and Figure 9. In this case, note that the forces are larger and that the wave forces in general add the major contribution in the B mooring. This is due to the up-stream localization of these moorings (with this wave and current heading). In the crowfoot type mooring, note also that the forces are increase by approximately 3 when waves are accounted for.

Overall this means that both waves and current are of importance and must be considered in a design approach.

4.3 *Irregular waves*

In NS 9415, it is specified that when using a design wave approach the wave height should be

$$H_{max} = 1.9\ Hs$$

Where H_{max} is the design wave height and Hs is the significant wave height of the sea state. Fish farms are in general large in horizontal extension. Forces in a given part of the mooring system may be due to the interaction of forces transported within the whole system. This means that in a design wave approach, there may be many wave crests along the facility. This may give conservative results. In this section this is investigated.

The structure is responding strongly nonlinear with respect to applied load. This means that time series realizations of a sea state must be carried out for a realization of a sea state to account for irregular waves.

As time series will repeat after a given amount of time the two aspects are correlated. In the present study it was decided to discretize to 20 waves in the spectrum and have a length of each time series giving 20 wave cycles at Tp. A PM spectrum is used.

Table 3 shows the load cases applied for the irregular sea calculations.

Table 3 Load cases irregular seas

Case	Hmax/Hs [m]	Period [s]	Wave angle [deg.]	U [m/s]	Current angle [deg.]
1	2.85/1.5	4.23	-45	0.5	-10
2	3.8/2.0	5.1	-90	0.5	-80

For load case 1, 6 time series were generated using different random seeds, and for load case 2, 4 time series were generated.

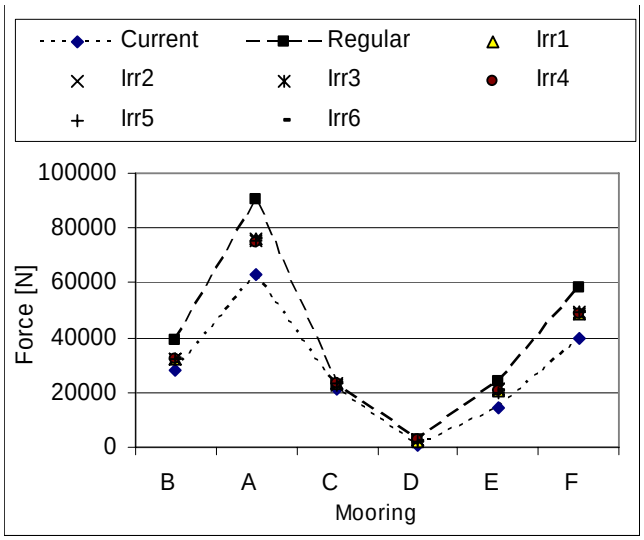

Figure 14 Forces in different parts of mooring system. Load case 1

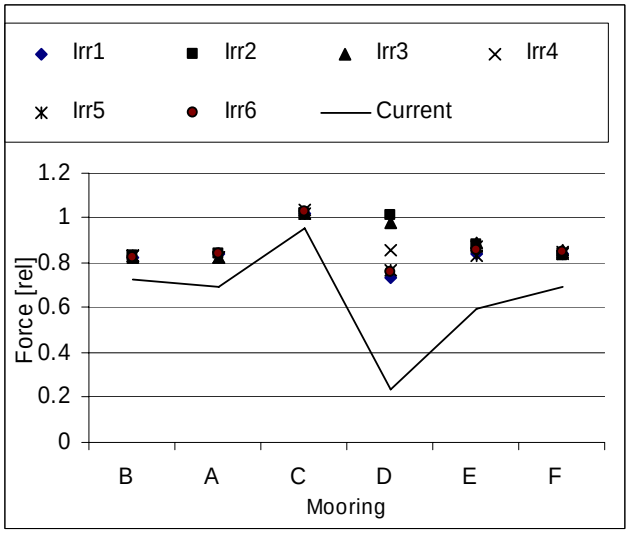

Figure 15 Forces in different parts of mooring system relative to forces calculated with a regular wave. Load case 1.

Figure 14 and Figure 15 show forces in the different parts of the mooring for load case 1. The label "Irr#" denotes load case # using irregular wave. The label "current" means that the structure is exposed to current only, whereas "Regular" means results calculated using a regular wave with wave height = 1.9Hs.

Figure 16 and Figure 17 shows the same as Figure 14 and Figure 15 respectively, but for load case 2.

As seen from Figure 14 - Figure 17 results using a regular wave is in general on the conservative side.

For mooring cables type A and B, the force increase due to waves is approximately half of the results for a regular wave.

Mooring cable C does not get that much axial forces and results using the two methodologies are similar.

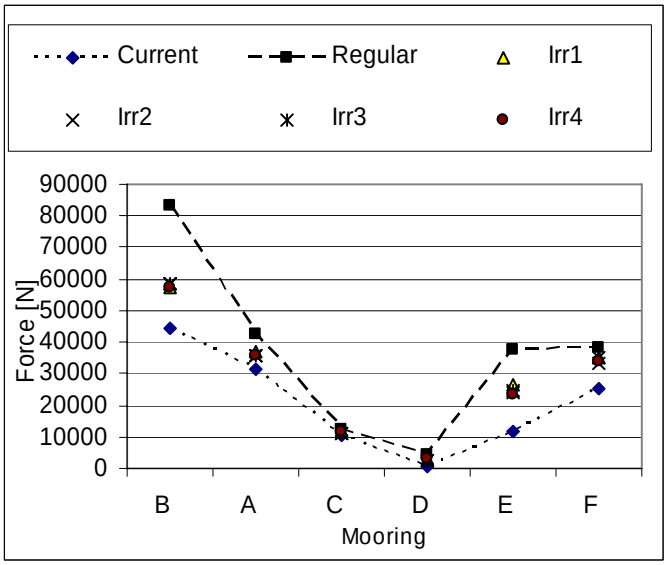

Figure 16 Forces in different parts of mooring system. Load case 2

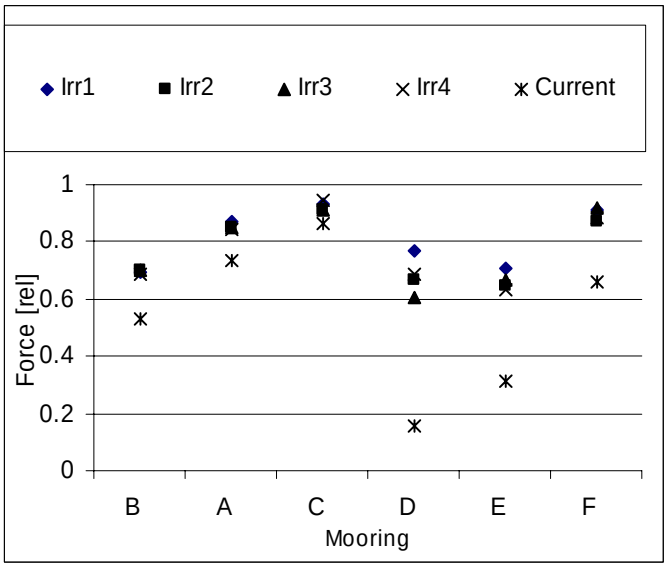

Figure 17 Forces in different parts of mooring system relative to forces calculated with a regular wave. Load case 2

In the vertical net staves (type D) forces from irregular waves are almost as large as the regular wave case. This may be explained by the fact that the net staves are more sensitive to forces acting locally in a very limited area.

For the Crowfoot type moorings (type E) forces are reduced slightly by introducing irregular seas, but the reduction is much less significant than for mooring cables type A and B. This may also be explained from the fact that they are more depending on forces over a limited area.

For the frame mooring (type F) the force increase due to waves are almost halved for load case 1, whereas it is only reduced with 24% for load case 2.

This means one should be careful to generalize force reductions.

5 CONCLUSIONS

Three different case studies have been carried out. Even though environmental load conditions changes a lot from location to location, the load conditions presented in the calculations represent typical conditions for the Norwegian fish farms industry.

The relation between applied current and forces in the mooring was investigated. The forces were non- linear with respect to current velocity and falling into the range between linear and square behavior biased toward square.

The significance of waves relative to current was investigated. Load components from both current and waves were found to be in the same order of magnitude. Hence their combined load contribution should be accounted for. For the net staves waves were most important. For the other moorings they were about equally important for this case study. This will vary depending on the environmental conditions at each location.

It is in general conservative to use a regular design wave approach based on wave height = 1.9Hs. The degree of conservatism ranged from 0 to 50%. In general, the conservatism was largest for the mooring cables connecting the frame to the sea bottom. However the design wave amplitude should not be reduced for the general case as the conservatism was found to vary strongly for load cases and components. More research effort should be put to this.

6 REFERENCES

Aarsnes, J. V., Løland, G and Rudi, H, (1990). "Current Forces on Cages, Net Deflection." Engineering for offshore fish farming, Glasgow, United Kingdom.

Berstad, A. J., H. Tronstad, and A. Ytterland, (2004)" Design Rules for Marine Fish Farms in Norway. Calculation of the Structural Response of such Flexible Structures to Verify Structural Integrity", Proceedings of OMAE 2004. Vancouver Canada. ASME (www.asme.org). Paper nr. OMAE-51577.

Berstad, A. J., Tronstad, H., Sivertsen and Leite (2005)" Enhancement of design criteria for fish farm facilities including operations", Proceedings of OMAE 2005. Halkidiki, Greece. ASME (www.asme.org). Paper nr. OMAE-67451.

Fredheim, A and O. F. Faltinsen (2003) "Hydroelastic analysis of a fishing net in steady inflow conditions", Hydroelasticity in Marine Technology, Oxford, UK.

Fredriksson, D.W., M.R. Swift, J.D. Irish, I. Tsukrov and B. Celikkol,(2003). "Fish Cage and Mooring System Dynamics Using Physical and Numerical Models with Field Measurements." Aquaculture Engineering, Vol. 27, No. 2, pp. 117-146.

Halse, K. H. (1997) "On Vortex Shedding and Prediction of Vortex-Induced Vibrations of Circular Cylinders." Phd. Thesis. Department of Marine Structures, Faculty of Marine Technology, Norwegian University of Science and Technology (NTNU).

Lader, P. F., B. Enerhaug, A. Fredheim and J. Krokstad (2003) "Modelling of 3D Net Structures Exposed to Waves and Current", Hydroelasticity in Marine Technology, Oxford, UK.

Lader, P. F. and B. Enerhaug. (1994) Experimental investigation of forces and geometry of a net cage in uniform flow. Accepted for publication in IEEE Journal of Ocean Engineering.

Løland, G. (1991) Current forces on and flow through fish farms. Phd Thesis. Department of Marine Hydrodynamics, Faculty of Marine Technology, Norwegian University of Science and Technology (NTNU).

NAS(2003): "NS 9415 Marine fish farms – requirements for design, dimensioning, production, installation and operation". Publisher: Standards Norway, Pronorm AS Postboks 252, 1322 Lysaker, Norway. http://www.standard.no.

Tronstad, H. (2000) "Nonlinear Hydroelastic Analysis and Design of Cable Net Structures Like Fishing Gear Based on the Finite Element Method" PhD thesis. Institute of Marine Technology NTNU, Trondheim.

Vikestad and Lien (2005) Proceedings of OMAE 2005. Halkidiki, Greece. ASME (www.asme.org). Paper nr. OMAE2005 - 67570